Falling Film Absorption on a Cylindrical Tube

A. T. Conlisk
Dept. of Mechanical Engineering, The Ohio State University, Columbus, OH 43210

The falling liquid film has become a popular means of transferring heat and mass from a vapor to a binary liquid film; applications include heat pump systems, desalination, and gas-liquid contactors. In the heat pump application, in particular, the length of the liquid film is a crucial factor because of size and weight limitations. Consequently, it is desirable to be able to predict the amount of mass absorbed in a given length of tube. In this work the absorption of water vapor into a Lithium-Bromide Water mixture is considered. It is shown that mass transfer takes place in a thin layer of fluid near the liquid-vapor interface which is indicative of a very high level of liquid-side mass-transfer resistance. Closed form solutions for the velocity field may be used to derive a simple closed form solution for the mass fraction. For very thin films the temperature distribution may be obtained analytically in Laplace transform space; however, due to the complexity of the solution, numerical techniques are employed to obtain quantitative results. For thicker films a closed form solution for the temperature may be obtained as well. The principal objective of this work is to develop a design procedure not requiring a significant amount of numerical work whereby the absorption capacity of a given tube may be predicted as a function of the governing geometrical and physical parameters. The analytical/numerical results are presented for parameters corresponding to those of recent experiments and the agreement between theory and experiment is good.

Introduction

The falling liquid film has become a popular means of transferring heat and mass from a vapor to a binary liquid film; applications include heat pump systems, desalination, and gas-liquid contactors. In the heat pump application, in particular, the length of the liquid film is a crucial factor because of size and weight requirements. Consequently, it is desirable to be able to predict the amount of mass absorbed in a given length of tube; thus the principal objective of this work is to develop a design procedure not requiring a significant amount of numerical work whereby the absorption capacity of a given tube may be predicted as a function of the governing geometrical and physical parameters. Because of its desirable thermodynamic properties and its widespread use in energy transfer equipment, the mixture of interest is Lithium-Bromide and Water (Buffington, 1949).

As a reference problem, consider the flow of a liquid in contact with its own vapor flowing vertically down a smooth cylindrical tube as depicted in Figure 1. For the case of a pure liquid, condensation of vapor at the interface produces a film thickness as shown in Figure 1. If the vapor is at constant pressure, then the temperature at the liquid-vapor interface usually corresponds to the saturation temperature at the liquid vapor pressure. Consider now the case of a binary liquid mixture in contact with a condensable vapor; further assume that the vapor corresponds to one (and only one) of the components of the liquid mixture. Then, again assuming constant vapor pressure, the absorption at the interface is controlled by a driving potential related to the difference between the interfacial mass fraction (say of species A) and the mass fraction in the bulk of the liquid film and a combination of parameters involving the Schmidt number. The precise structure of the flow and temperature fields near the liquid-vapor interface will be discussed later and a sketch of the likely concentration field is also depicted in Figure 1. What is clear from the present work is that the rate of absorption of the water to the film is strongly dependent on the local flow field. For the smooth tube of Figure 1, at the flow rates of interest, the flow is of the lubrication type and analytical closed-form solutions for the velocity field may be easily obtained outside the entrance region of the tube. The terms mass fraction and concentration

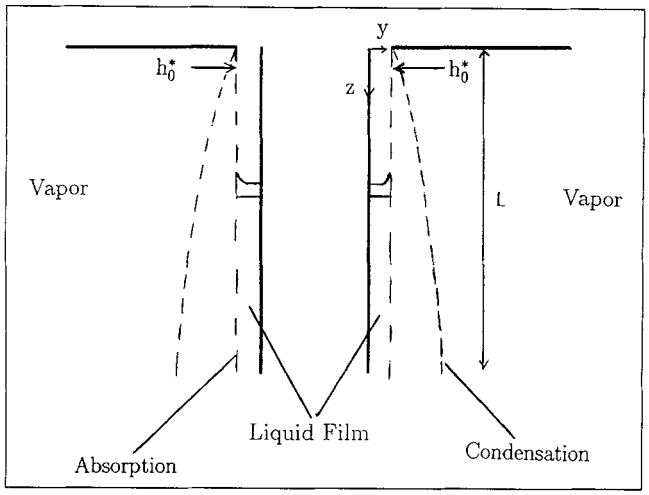

Figure 1. Cross-sectional view of the flow of a mixture down the outside of a cylindrical tube.

The large, liquid-side mass-transfer resistance forces the film thickness in the case of absorption to remain constant to leading order. Mass transfer takes place only in a thin layer near the liquid-vapor interface. The mass fraction profile shown is that of the absorbing species. The thickness of the liquid film is greatly expanded for clarity.

will be used interchangeably with the governing equations formulated in terms of mass fraction or weight percent.

Colburn and Drew (1937) consider the condensation of a binary mixture on a surface; however they did not consider the effect of the flow field on the condensation problem and their results rely solely on thermodynamic considerations. Sparrow and Marschall (1969) consider the condensation of a binary mixture on a vertical surface as well; the vapor flow is driven by the condensation and the vapor Reynolds number is large; consequently, the vapor flow is of boundary layer type. They did not consider the liquid film flow problem and they assume that the mass fraction difference across the liquid film is negligible.

Olbrich and Wild (1969) consider the absorption of a gas into a liquid for the case where the gas absorption rate is very low (see also Rotem and Neilson (1969)); Tamir and Taitel (1971) consider the effect of mass-transfer resistance at the surface of the film and model the film surface condition using a mass-transfer coefficient approach. Grossman (1983) considers the absorption of a vapor into a liquid binary mixture. He suggests that at low absorption rates the film thickness remains constant to leading order, and he obtains a solution for the species mass fraction in the liquid film both numerically and using an eigenfunction expansion technique. In Grossman (1987) the results are generalized to the case where back-diffusion occurs; that is, concentration or mass fraction differences affect the energy equation. Recently van der Wekken and Wassenaar (1988) have generalized the problem of Grossman (1983) to include more complex boundary conditions at the wall and at the interface; they also neglect the effect of film thickness variation. Uddholm and Setterwall (1988) consider the effect of a wavy film profile so that the film thickness is not constant. Their design procedure is subject to the specification of several experimentally determined parameters. Andberg and Vliet (1983) numerically compute the solution for the absorption of LiBr into water at very low flow rates and include an enthalpy transport term in the energy equation; the mass transport equation is formally equivalent to the equation solved by Grossman (1983) and because of the low flow rate, mass transfer takes place over the entire film. Grigor'eva and Nakoryakov (1977) consider essentially the same problem as Grossman (1983) and Andberg and Vliet (1983) using an eigenfunction expansion technique. In all this work, the tube is assumed to be smooth and the film thickness is taken to be constant based on physical reasoning that the amount of fluid absorbed into the film is likely to be small. In addition, equilibrium is assumed to hold at the interface.

In the present work, we also assume equilibrium obtains at the liquid-vapor interface and show that there is a large liquid-side resistance which is the major controlling factor in determining the rate of absorption of vapor into the liquid film. We show that, in fact for large Schmidt number, mass transfer takes place only in a very thin region near the interface and this may be one reason absorption rates are very low. Moreover, the assumption of a constant film thickness in the absorption problem which appears incorrect at first glance may be justified as a consequence of the very large liquid-side resistance. The validity of this assumption depends on the magnitude of a suitably defined mass-transfer driving parameter and on the fact that the Schmidt number is large; this mass-transfer driving parameter appears to have been discussed first by Merk (1959) and later by Acrivos (1962).

The usual balance for mass transfer in many systems states that Fick diffusion is balanced by convection of the bulk fluid (Bird, Stewart and Lightfoot, 1960). The driving potential for the classical Fick diffusion is a mass fraction or concentration gradient and the proportionality constant is the diffusion coefficient. It will be assumed here that Fick diffusion balances the bulk convection of mass and the fluid properties are assumed to be constant. In this case the convective terms in the mass-transfer equation are proportional to $\epsilon ReSc$ where Sc is the Schmidt number, $Sc=\nu/_{D_{AB}}$, Re is the Reynolds number, $Re=(U_0h_0^*)/\nu$, and $\epsilon=h_0^*/L$ is small (see the section on fluid mechanics); for liquids $Sc\gg 1$. Thus, for ϵRe not too small, any mass transfer is confined to the region immediately adjacent to the free surface of the liquid film.

The absorption rate is also dependent on the overall driving potential for Fick's law. The overall driving potential is characterized by the overall difference between the surface mass fraction and the mass fraction in the bulk of the film. The parameter which characterizes this potential is

$$B=\frac{\omega_{AS}-\omega_{A\,BULK}}{1-\omega_{AS}} \tag{1}$$

where ω_{AS} may be identified with the surface mass fraction at the inlet of the tube; for $B\ll 1$ and $\epsilon ReSc\gg 1$ it can be shown that the film thickness is constant to leading order and very little mass transfer will take place. In this article for the lithium-bromide-water mixture of interest $\delta=1/(\epsilon ScRe)\ll 1$.

The plan of this article is as follows. First, solutions for the flow and the heat and mass transfer are derived in the limit of mass-transfer-driving parameter $B\to 0$ in the thin film, lubrication limit. Then, solutions are obtained for the case of $\epsilon Re=0(1)$, and their results are compared with recent experimental measurements.

The Thin Film Limit

Fluid mechanics

In the present work, the flow field is of the lubrication type with the film thickness slowly varying in the direction of gravity (that is, the vertical direction). The physical situation is depicted in Figure 1; here the film is extremely thin, is driven by gravity, and the pressure gradient across the film is thus negligible. In this case the velocity field in dimensionless form is given by:

$$u = -\epsilon ReFry^2 h_z/2 \tag{2}$$

$$w = FrRe(yh - y^2/2) \tag{3}$$

where $\epsilon = h_0^*/L$, $Fr = gh_0^*/U_0^2$ is a Froude number and $h_z = dh/dz$. Here all distances normal to the wall have been normalized on the initial film thickness h_0^* and the axial coordinate has been normalized on the length of the tube. The Reynolds number in Eqs. 2 and 3 is the Reynolds number based on the initial film thickness and the average velocity based on the required flow rate. The dimensional mass flow rate in the axial direction down the tube is:

$$\dot{m}^* = 2\pi r_i \rho \int_0^{h_0^*} w^* dy \tag{4}$$

where r_i is the radius of the tube and in dimensionless form:

$$\dot{m} = FrReh^3/3 \tag{5}$$

where

$$\dot{m} = \dot{m}^*/(2\pi r_i \rho h_0^* U_0) \tag{6}$$

and $\dot{m}^*$ is dimensional. It should be noted that from the point of view of the absorption problem the velocity field should be interpreted as the mass averaged velocity of the mixture. To determine the appropriate values of h_0^* and U_0 given the flow rate, the definition of $\dot{m}^*$ at the inlet specifies the product $U_0 h_0^*$; in addition, the average velocity U_0 is related to h_0^* through the Nusselt relation $U_0 = gh_0^{*2}/\nu$ and these two equations thus fix U_0 and h_0^*.

Now, in dimensionless form:

$$d\dot{m}/dz = FrReh^2 dh/dz \tag{7}$$

and by a mass balance at the interface the amount of fluid absorbed is given by:

$$\dot{m}_a = -d\dot{m}/dz = u_0 - wdh/dz \tag{8}$$

where $u_0 + \epsilon u + \ldots$ and where the negative sign indicates that the velocity of the fluid into the film is in a direction opposite to the outward unit normal to the liquid film surface. Equation 8 is valid for the case where the condensing fluid has the same composition as the mixture fluid. Most often this is not the case and the actual amount of water condensed or absorbed in terms of the mixture properties $\alpha\dot{m}_a$ is where $\alpha = \rho_w/\rho$ where ρ_w is the density of water in the bulk.

Temperature distribution

The dimensionless form of the energy equation for the present problem is:

$$\epsilon RePrh\left[(u_0 - h_z w)\frac{\partial T}{\partial \eta} + hw\frac{\partial T}{\partial z}\right] = \frac{\partial^2 T}{\partial \eta^2} \tag{9}$$

where Pr is the Prandtl number $Pr = \mu c_p/k$, and $\eta = y/h$. We assume that in the present problem, for $\epsilon Re \ll 1$, $\epsilon RePr \sim 1$ and so the convective terms balance the conduction terms in Eq. 9. We nondimensionalize the temperature as:

$$\theta = \frac{T - T_{\text{win}}}{T_{\text{sin}} - T_{\text{win}}} \tag{10}$$

where T_{sin} is the film surface temperature at the top of the tube and T_{win} is the wall temperature there. Anticipating from the analysis of the section on mass transfer that the film thickness is constant to leading order ($u_0 = 0$; $h = 1 + \ldots$) then we write Eq. 9 as:

$$\frac{\partial^2 \theta}{\partial \eta^2} = \lambda w \frac{\partial \theta}{\partial z} \tag{11}$$

where $\lambda = \epsilon RePr = 0(1)$; the boundary conditions are:

$$\theta = \theta_w \quad \text{at} \quad \eta = 0 \tag{12}$$

and

$$\frac{\partial \theta}{\partial \eta} = -\frac{\alpha \dot{m}_a}{Ja}\epsilon RePr \quad \text{at} \quad \eta = 1 \tag{13}$$

and the initial condition is assumed to be $\theta = 0$ at $z = 0$. Here Ja is the Jakob number which is defined by $Ja = (c_p \Delta T)/h_{\text{abs}}$ where c_p is the constant pressure specific heat; $\Delta T = T_{\text{sin}} - T_{\text{win}}$ and h_{abs} is the heat of absorption. We solve Eq. 11 using the Laplace transform in z. Let $\xi = 1 - \eta$; then after taking the Laplace transform we have:

$$\frac{\partial^2 \hat{\theta}}{\partial \xi^2} = \frac{\lambda_1 s}{2}(1 - \xi^2)\hat{\theta} \tag{14}$$

where s is the transform variable and $\lambda_1 = \lambda ReFr$. The boundary conditions are:

$$\frac{\partial \hat{\theta}}{\partial \xi} = H\hat{\dot{m}}_a \quad \text{at} \quad \xi = 0$$
$$\hat{\theta} = \hat{\theta}_w \quad \text{at} \quad \xi = 1 \tag{15}$$

where $H = \alpha\lambda/Ja$.

The solution to Eq. 14 may be obtained in terms of parabolic cylinder functions; the solution in the transformed plane is complicated and the inversion of the transforms generated cannot be easily obtained. Thus for the purpose of presenting the results, a numerical solution was obtained (see the section on numerical solution for the temperature). However, since the heat- and mass-transfer fields are intimately coupled in a rather complicated way, the analytical procedure is illustrative

of the closure process and determination of the leading order film thickness variation. Thus, let

$$\hat{\theta} = e^{i\sqrt{a}\xi^2} f \tag{16}$$

where $a = \lambda_1 s/2$. Then f satisfies:

$$f'' = xf' + cf = 0 \tag{17}$$

where the prime denotes differentiation by $x = \xi/2i\sqrt{a}$ and $c = -1/4a(i\sqrt{a} - a)$. The general solution to Eq. 17 is given by Gradsteyn and Rhyzhik (1980, p. 1067) as in the present notation:

$$f = e^{-x^2/4} D_{c-1}(\pm x) \tag{18}$$

where D_{c-1} is the parabolic cylinder function of order $c-1$. The two solutions $D_{c-1}(\pm x)$ are linearly independent. Thus,

$$\hat{\theta} = e^{(i\sqrt{a}\xi^2/2 - \xi^2/4a)}\{A_1 D_{c-1}(\xi/2i\sqrt{a}) + B_1 D_{c-1}(-\xi/2i\sqrt{a})\} \tag{19}$$

where A_1 and B_1 are arbitrary constants. The solution, Eq. 19, may also be obtained by seeking a solution in terms of the general integral form:

$$f = \int_C e^{px} g(p)\, dp.$$

To satisfy the boundary conditions we have:

$$\hat{\theta}_w = e^{(i\sqrt{a}/2 - 1/4a)}\left\{A_1 D_{c-1}\left(\frac{1}{2i\sqrt{a}}\right) + B_1 D_{c-1}\left(\frac{-1}{2i\sqrt{a}}\right)\right\} \tag{20}$$

and

$$A_1 - B_1 = \frac{2i\sqrt{a} H \hat{m}_a}{D_0} \tag{21}$$

where $D_0 = D'_{c-1}(0)$. Equations 20 and 21 are two equations in two unknowns for A_1 and B_1 which are defined by:

$$A_1 = \frac{\hat{\theta}_w e^{(1/4a - i\sqrt{a}/2)} - 2i\sqrt{a} H \hat{m}_a \dfrac{D_+}{D_0}}{D_+ + D_-} + 2i\sqrt{a} H \hat{m}_c$$

$$B_1 = \frac{\hat{\theta}_w e^{(1/4a - i\sqrt{a}/2)} - 2i\sqrt{a} H \hat{m}_a \dfrac{D_+}{D_0}}{D_+ + D_-} \tag{22}$$

where

$$D_+ = D_{c-1}\left(\frac{1}{2i}\sqrt{a}\right)$$

$$D_- = D_{c-1}\left(-\frac{1}{2i}\sqrt{a}\right).$$

We have then

$$\hat{\theta} = \frac{\hat{\theta}_w e^{(1/4a - i\sqrt{a}/2)(1-\xi^2)}}{D_+ + D_-}\left\{D_{c-1}\left(\frac{\xi}{2i\sqrt{a}}\right) + D_{c-1}\left(\frac{-\xi}{2i\sqrt{a}}\right)\right\}$$
$$- 2i\sqrt{a} H \hat{m}_a e^{(1/4a - i\sqrt{a}/2)\xi^2}\left\{\left(\frac{D_+}{D_0(D_+ + D_-)} - 1\right) D_{c-1}\left(\frac{\xi}{2i\sqrt{a}}\right) + \frac{D_+}{D_0(D_+ + D_-)} D_{c-1}\left(-\frac{\xi}{2i\sqrt{a}}\right)\right\} \tag{23}$$

and note that at the interface,

$$\hat{\theta}_s = 2\hat{\theta}_w \frac{D_{c-1}(0)}{D_+ + D_-} e^{(1/4a - i\sqrt{a}/2)} \times \frac{-2i\sqrt{a} H \hat{m}_a D_{c-1}(0)}{D_0}\left\{\frac{2D_+}{(D_+ + D_-)} - 1\right\}. \tag{24}$$

The two physical effects acting to change θ_s are now clear from Eq. 24; if θ_w is not constant, then θ_s will change; secondly if $\dot{m}_a$ is not constant (even when θ_w is constant) θ_s will also change. We will use Eq. 24 in the calculation of the leading order film thickness variation to be discussed in the section on interfacial conditions.

As noted earlier, the expressions, Eqs. 23 and 24 are too complicated to yield to readily identifiable simple, real valued solutions. Thus, a numerical solution was sought to present the results and this solution is discussed later. At this point, pending discussion of the numerical solution for the temperature field we now consider the mass-transfer problem.

Mass transfer

Let A denote the mass fraction of water in the mixture. Then with $\eta = y/h$, the governing equation of mass transfer is given by

$$h\left\{(u_0 - h_z w)\frac{\partial \omega_A}{\partial \eta} + hw\frac{\partial \omega_A}{\partial z}\right\} = \delta \frac{\partial^2 \omega_A}{\partial \eta^2} \tag{25}$$

subject to

$$\frac{\partial \omega_A}{\partial \eta} = 0 \quad \text{at} \quad \eta = 0 \tag{26}$$

$$\delta \frac{\partial \omega_A}{\partial \eta} = -\alpha \dot{m}_a h(1 - \omega_A) \quad \text{at} \quad \eta = 1. \tag{27}$$

Here $\delta = (\epsilon ReSc)^{-1} \ll 1$ for the parameters of the problem. Thus it is expected that any mass transfer will be confined to a thin layer near the liquid-vapor interface.

To deduce the structure of the solution we scale ω_A and define

$$\Omega = \frac{\omega_A - \omega_{A\,\text{BULK}}}{\omega_{A\,\text{sin}} - \omega_{A\,\text{BULK}}} \tag{28}$$

where $\omega_{A\,\mathrm{sin}}$ is the mass fraction of species A at the interface at the inlet. In terms of Ω, the boundary condition at the interface becomes

$$\delta B\frac{\partial\Omega}{\partial\eta}=-h\alpha\dot{m}_a+0(B)\quad\text{at}\quad\eta=1. \tag{29}$$

The parameter range of practical interest in this work was described earlier; the small value of B further increases the liquid side mass-transfer resistance at the interface. In this case Eqs. 25-27 may be written in scaled variables according to $(\bar{\eta}=(1-\eta)/\delta^{1/2})$,

$$\frac{\partial^2\Omega}{\partial\bar{\eta}^2}=h^2w\frac{\partial\Omega}{\partial z}-B/\alpha\frac{\partial\Omega}{\partial\bar{\eta}}\bigg|_{\eta=0}\frac{\partial\Omega}{\partial\bar{\eta}} \tag{30}$$

with

$$\delta^{1/2}B\frac{\partial\Omega}{\partial\bar{\eta}}=\alpha h\dot{m}_a\quad\text{at}\quad\bar{\eta}=0. \tag{31}$$

Equation 30 balances for $B\to 0$; however the boundary condition at $\bar{\eta}=0$ does not. The conclusion which must be reached is that since B and δ are both small, then

$$\dot{m}_a\sim\delta^{1/2}B \tag{32}$$

that is, the lack of an $O(1)$ mass fraction difference and the fact that δ is small limits the amount of absorption at the interface. Since, from Eqs. 7 and 8 $\dot{m}_a$ is proportional to the slope of the interface, the magnitude of dh/dz is severely limited. Thus, to leading order, we may take $h=1$. Moreover, the second term on the right side of Eq. 30 may be neglected for B small, unless it is to be noted, α is also small. This is apparently the parameter range considered by Grossman (1983) although he assumes that mass transfer takes place over the entire film.

The solution to Eq. 30 subject to the indicated boundary conditions and an initial condition may be obtained using the Laplace Transform; the solution may be expressed as a convolution of $\dot{m}_a$ with the fundamental solution of the system and a detailed solution then depends on the actual calculation of leading order nonzero term in $\dot{m}_a$. The solution to this problem subject to the initial condition $\Omega=0$ at $z=0$ and $\Omega=0$ as $\bar{\eta}\to\infty$ is given by

$$\Omega=-\alpha\{2/(ReFr\pi)\}^{1/2}\int_0^z\dot{m}_{a0}(z-t)e^{-ReFr\bar{\eta}^2/8t}dt/t^{1/2} \tag{33}$$

where $\dot{m}_{a0}$ is the leading order nonzero term in the absorbed flux. Here

$$m_{a0}=-ReFr\frac{dh_1}{dz} \tag{34}$$

where

$$h=1+\delta^{1/2}Bh_1+\ldots. \tag{35}$$

For eventual comparison with experiment we calculate the average mass fraction:

$$\Omega_{\mathrm{AVE}}=\delta^{1/2}\int_0^\infty\Omega d\bar{\eta}=2\delta^{1/2}\alpha h_1$$

where h_1 is defined in Eq. 35. We now move to a discussion of the interfacial conditions from which we can calculate h_1.

Interfacial conditions

The boundary condition at the interface reveals an intimate connection between the temperature and concentration (that is, mass fraction) fields. Assuming that only conduction is important at the interface, as noted previously

$$\frac{\partial\theta}{\partial\eta}=-\alpha\dot{m}_a\epsilon RePr/Ja \tag{36}$$

and from Eq. 29 (for $h=1$ to leading order) we note

$$\frac{\partial\theta}{\partial\eta}=(BLe/Ja)\frac{\partial\Omega}{\partial\eta} \tag{37}$$

at the interface, where $Le=Pr/Sc$ is the Lewis number and Ja is the Jakob number defined previously. As expected, the temperature gradient at the interface is inversely proportional to the Schmidt number and as $Sc\to\infty$ no heat transfer, and consequently no mass transfer will take place. Equation 37 would seem to imply that a balance occurs for $BLe/Ja=O(1)$ which then gives a rough estimate for the value of B in terms only of the properties of the mixture and of the overall temperature gradient across the film. However, the regions over which heat and mass transfer take place near the interface are different and the independent variables must be scaled appropriately. In the present case the parameter $\delta_1=(\epsilon RePr)^{-1}$ is assumed to be $O(1)$, and the only small scale is that of the mass-transfer layer. This results in the condition

$$\frac{\partial\theta}{\partial\eta}\bigg|_{\eta=1}=-BLe\delta^{-1/2}/Ja\frac{\partial\Omega}{\partial\bar{\eta}}\bigg|_{\bar{\eta}=0}. \tag{38}$$

Theoretically, Eq. 38 then determines the film thickness; however, the dimensionless interface temperature θ_s is also unknown and hence another condition is required to close the problem. All previous work in this area assumes that equilibrium obtains at the interface and we assume that this is the case here.

We assume a linear absorbent (Grossman, 1983) and in dimensional form,

$$\omega_{AS}=C_1T_s+C_2 \tag{39}$$

where C_1 and C_2 are constants particular to the absorbent. In dimensionless form,

$$\Omega_s=\frac{C_1\Delta T}{\Delta\omega}\theta_s+\beta$$
$$\Delta T=T_{\mathrm{sin}}-T_{\mathrm{win}},\quad\beta=\frac{C_1T_w+C_2-\omega_{A\,\mathrm{BULK}}}{\Delta\omega}. \tag{40}$$

Equations 40 provide the link between the film surface temperature and the surface mass fraction.

We illustrate the solution for the film thickness using the solution for the temperature field at the interface from Eq. 24; first using the solution to the mass-transfer problem, we note that in transform space

$$\hat{\Omega}_s = \alpha\sqrt{2ReFrs}\,\hat{h}_1. \tag{41}$$

Taking the transform of Eq. 40 and substituting the solution for the surface temperature we obtain

$$\hat{h}_1\left\{1 - \frac{iC_1\Delta T\lambda ReFr\dfrac{BLe^{1/2}}{Ja}}{\Delta\omega D_0} \times D_{c-1}(0)e^{(1/4a - i\sqrt{a}/2)}\left\{\frac{2D_+}{(D_+ + D_-)} - 1\right\}\right\} = \frac{2C_1\Delta T\hat{\theta}_w D_{c-1}(0)e^{(1/4a - i\sqrt{a}/2)}}{\alpha\Delta\omega\sqrt{2ReFrs}\,(D_+ + D_-)} + \frac{\hat{\beta}}{\alpha\sqrt{2ReFrs}} \tag{42}$$

which is a single equation for $\hat{h}_1$. If $\hat{\theta}_w = 0$ (that is, θ_w = constant) and we neglect the constant on the left side of Eq. 42 with respect to 1, then

$$h_1 \sim \frac{\beta}{\alpha}\sqrt{\frac{2z}{ReFr\pi}} \tag{43}$$

which is the typical boundary layer behavior $h_1 \sim z^{1/2}$.

The temperature and mass fraction at the interface are related by the equilibrium condition and by the similarity of the boundary conditions at the interface. Using Eqs. 24, 40 and 41 this relationship is given by, in the transformed plane

$$\hat{\theta}_s = \frac{BLe^{1/2}}{Ja}G(s)\hat{\Omega}_s \tag{44}$$

where the subscripts in Eq. 44 denote surface quantities and G is a complicated function of the Laplace inversion variable which is also denoted by s. In the boundary layer limit $G(s) = 1$ (see below) and the relationship is particularly simple: $\theta_s = [(BLe^{1/2})/Ja]\Omega_s$.

In principle, Eq. 42 for the transform of h_1 could be inverted to obtain the leading order film thickness variation; however it is clear that such an inversion process would yield an extremely complicated solution for h_1. Consequently a numerical solution for the temperature field was sought and this is discussed next.

Numerical solution for the temperature

As mentioned earlier, the inversion of the solution for the temperature field in transform space is too complicated to be obtained analytically; consequently a numerical solution to the transform problem was sought. Using the first of Eqs. 40 and Eq. 41, the boundary condition at the interface may be written as

$$\frac{\partial\hat{\theta}}{\partial\xi} = \frac{\epsilon RePrA}{Ja}\left\{\frac{C_1\Delta T}{\Delta\omega}\hat{\theta} + \hat{\beta}\right\}, \text{ at } \xi = 0 \tag{45}$$

where A is defined by

$$A = -\frac{(ReFrs\delta)^{1/2}B}{\sqrt{2}}.$$

With closure effected by the equilibrium condition, the problem corresponding to Eq. 14, subject to Eq. 45, and the second of Eqs. 15 is a standard ordinary differential equation in the complex domain. Discretization of Eq. 14 was done using standard central differencing in ξ; $N = 41$ points across the film was sufficient to insure three figure accuracy in the solution. The linear system generated by the discretization was solved by a standard elimination procedure. The corresponding solution for the dimensionless temperature θ was obtained by numerically evaluating the Laplace inversion integral

$$\theta = \int_{\alpha_0 - i\infty}^{\alpha_0 + i\infty}\hat{\theta}e^{sz}ds$$

for each value of ξ and z where α_0 is a real parameter $\alpha_0 > 0$ using the method described by Honig and Hirdes (1984). The parameters Re, Fr, Pr, C_1 and ΔT correspond to the physical parameters of the experiments of Miller (1991) who investigated the absorption of water into a lithium-bromide mixture; the parameters are summarized in Table 1. The values of C_1 and C_2 associated with the equilibrium properties of the mixture are discussed in the conclusion section.

Before discussing solutions to this problem, in the next section we consider the case where $\epsilon RePr \gg 1$ and significant heat transfer takes place only near the film interface.

The Boundary Layer Limit

The convective terms in the governing equations for flow in the liquid film become important when $\epsilon Re = O(1)$. In this case, the parameter $\delta \ll 1$, again. Thus, to leading order, the film thickness is still constant and Eqs. 2 and 3 are still valid with $h = 1 + O(\delta^{1/2}B)$. That is the convective terms vanish because:

$$\frac{\partial w}{\partial z} = 0$$

to leading order.

The fact that $\epsilon Re = O(1)$ affects the heat-transfer problem

Table 1. Experimental Parameters and Fit Constants C_1 and C_2

Data Set	1	2	3
Mass flux in (kg/min)	0.3728	0.5018	0.3590
Solution temperature in (K)	313.4	308.02	328.0
Mass fraction Libr in	0.5612	0.5633	0.6261
Absorber pressure (torr)	21.2	10.86	9.83
Reynolds number	30.86	31.31	20.15
Prandtl number	15.47	20.82	21.16
Schmidt number	1,626	2,460	2,425
Lewis number	0.0095	0.0085	0.0087
Froude number	0.0324	0.0320	0.0496
Jakob number	0.0085	0.0051	0.00054
C_1	−0.0065	−0.0056	−0.0049
C_2	2.5815	2.2118	1.9891

significantly, however. For most mixtures of interest in absorption the Prandtl number $Pr \gg 1$ and so for $\epsilon Re = 0(1)$, $\delta_1 = (\epsilon RePr)^{-1} \ll 1$; this suggests that as with the mass-transfer problem, heat transfer takes place in a thin layer near the interface of width $O(\delta_1^{1/2})$. The dimensionless temperature distribution may be found in the same way as the mass-transfer problem and the result is:

$$\theta = -\frac{2^{1/2}\alpha Le^{1/2}B}{\sqrt{ReFr\pi Ja}} \int_0^z \dot{m}_{a0}(z-t)e^{-\hat{\eta}^2 ReFr/8t} dt/t^{1/2} \tag{46}$$

where θ is now defined by:

$$\theta = \frac{T - T_{\text{BULK}}}{T_{\text{sin}} - T_{\text{BULK}}}$$

and $\hat{\eta} = (1-\eta)/\delta_1^{1/2}$; T_{BULK} is analogous to $\omega_{\text{A BULK}}$ and has been assumed to be constant. Evaluating Eq. 46 at $\hat{\eta} = 0$, and comparing with the mass-transfer solution given by Eq. 33 we find:

$$\theta_s = \frac{BLe^{1/2}}{Ja}\Omega_s. \tag{47}$$

Using the equilibrium condition as before we find that:

$$\Omega_s = \frac{(C_1 T_{\text{BULK}} + C_2 - \omega_{\text{A BULK}})/\Delta\omega}{1 - \dfrac{C_1 \Delta T}{\Delta\omega}\dfrac{BLe^{1/2}}{Ja}} \tag{48}$$

and thus if the bulk temperature is constant Ω_s is also constant. Note that the restriction $\Omega_s \geq 0$ places strict limits on the operating bulk temperature and mass fraction based on the physical constants C_1 and C_2.

To determine the leading order film thickness variation we can immediately invert Eq. 41 and the result is:

$$h_1 = \frac{1}{\alpha\sqrt{2ReFr\pi}} \int_0^z \Omega_s(t) \frac{dt}{\sqrt{z-t}} \tag{49}$$

for $T_{\text{BULK}} = \text{constant}$, Ω_s is constant and we obtain an equation similar to Eq. 43 with equality:

$$h_1 = \frac{\Omega_s}{\alpha}\sqrt{\frac{2z}{ReFr\pi}}. \tag{50}$$

Note the dependence of the surface mass fraction on the bulk temperature within the film. If T_{BULK} varies, then Ω_s will vary and the mass flux will vary as well. That is, conditions in the bulk of the liquid film can significantly affect the absorption process.

The behavior of the leading order film thickness variation in Eq. 50 is typical of classical boundary layer behavior. Note that because of this there is a singularity in the absorption mass flux near $z = 0$ $\{\dot{m}_{a0} \sim z^{-1/2},\ z \to 0\}$; this (integrable) singularity is purely local in character and may be removed by the calculation of a solution valid near $z = 0$, $\eta = 1$. However, since the mass fraction may be obtained in closed form, there is no need to perform such an additional calculation.

Results and Comparison with Experiments

A series of results for two sets of wall temperature profiles have been calculated; we first consider the case of constant wall temperature in which $\theta_w = 0$ at $\xi = 1$; next we consider the case of variable wall temperature in which

$$\theta_w = \frac{\Delta T_{\text{wall}}}{\Delta T} z^{1/2}. \tag{51}$$

In Eq. 51 ΔT_{wall} is a parameter to be specified and is the overall temperature difference between the inlet and the outlet at the wall. This distribution is a good approximation for the wall temperature distribution for the experimental results of Miller et al. (1992) as calculated by Perez-Blanco (1992); see below.

The properties of the fluid are taken from the results of Miller (1991, 1992) and each of the dimensionless parameters is calculated using properties averaged between the inlet and the outlet of the tube. The equilibrium coefficients C_1 and C_2 are obtained from curve-fits of the equilibrium data for $LiBr - H_2O$ mixtures given in the 1981 Heat Transfer Fundamentals Handbook (Figure 34, p. 17.72). It should be noted that in general, the mass fraction does not behave linearly with temperature; however, in the restricted ranges of interest here, the relationship is substantially linear. The coefficients C_1 and C_2 are also given on Table 1.

The experimental data has been generated by Miller (1991, 1992) at Oak Ridge National Laboratories. The test section consists of a five ft long, 3/4 in. outside diameter stainless steel tube. A series of tests at a number of values of solution flow rate and weight-percent lithium bromide were conducted. The test stand is instrumented at various locations for measurement of temperature, pressure, density, and flow rate. Inlet and outlet solution bulk temperatures were measured using an insertion probe. Absorber pressure was measured using Heise noncontacting optical sensors. A coriolis mass-flow meter and densitometer were used to measure solution flow rate and density, respectively. The inlet and outlet mass fractions based on density measurements were checked using a refractometer. Subsequent to the calculation of the mass-transfer quantities, the required wall temperature may be calculated and this data has been provided by Perez-Blanco (1992).

To determine the interface mass fraction at the entrance to the tube, we use the definition of Ω and Eq. 47 which relates the interfacial temperature and mass fraction; note that Eq. 47 is for the parameter range $\epsilon RePr \gg 1$. However, since the variation of the solutions in z is rather slow, the precise form of $G(s)$ in Eq. 44 is not crucial. Thus, using the definition of B in Eq. 48, assuming the bulk properties are constant, we have ($\Omega_{\text{sin}} = 1$):

$$\omega_{\text{A sin}}^2 - \left(1 + \omega_{\text{A BULK}} + \beta - C_1 \frac{Le^{1/2}h_{\text{abs}}}{c_p}\right)\omega_{\text{A sin}} + \omega_{\text{A BULK}} + \beta - C_1 \frac{Le^{1/2}h_{\text{abs}}}{c_p}\omega_{\text{A BULK}} = 0. \tag{52}$$

Equation 52 specifies the surface mass fraction of water at the inlet of the tube; β is defined by the third of Eqs. 40. Given $\omega_{\text{A BULK}}$, then the parameter B is determined; from the definition of the average mass fraction ω_{AVE} is given by

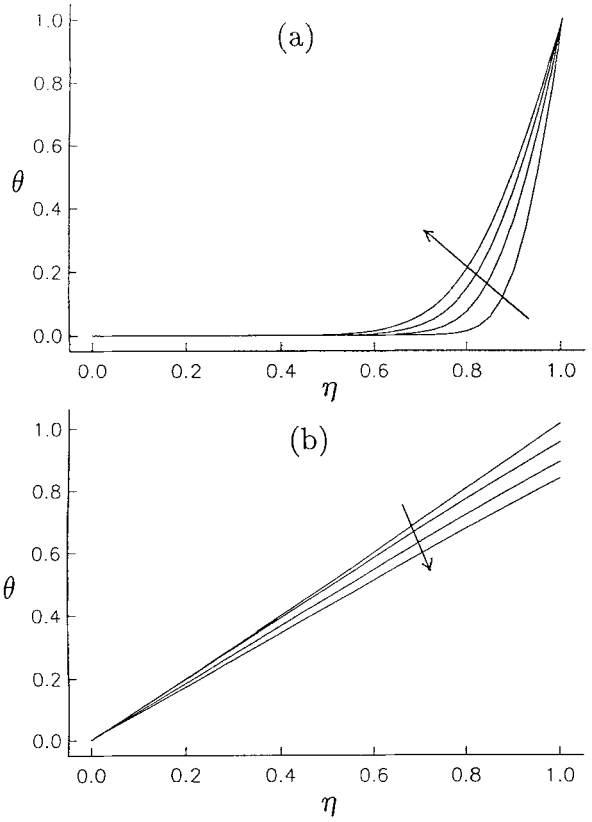

Figure 2. Dimensionless temperature distribution across the film for various values of z : flow rate = 3.728 kg/min.

Other parameters are for data set 1 of Table 1. The wall temperature is constant. (a) $z=0.0025$, 0.005, 0.0075, 0.01, and (b) $z=0.25$, 0.5, 0.75, 1.0. Arrow denotes direction of increasing z.

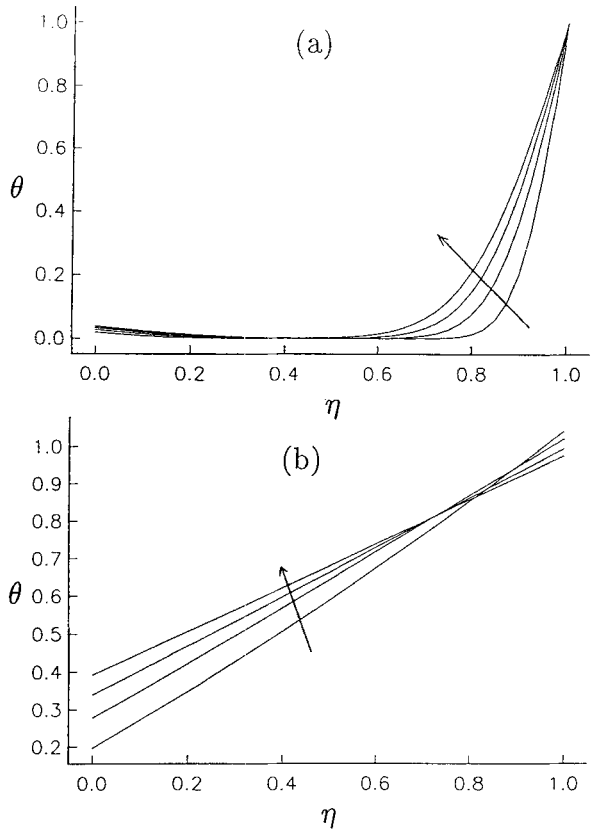

Figure 3. Dimensionless temperature distribution across the film for various values of z : flow rate = 3.728 kg/min.

Other parameters are for data set 1 of Table 1. The wall temperature is variable according to Eq. 51 with $\Delta T_{wall}=4$ K. (a) $z=0.0025$, 0.005, 0.0075, 0.01, and (b) $z=0.25$, 0.5, 0.75, 1.0. Arrow denotes direction of increasing z.

$$\omega_{AVE}=\omega_{A\,BULK}+2\alpha\Delta\omega\delta^{1/2}h_1. \tag{53}$$

In the experiments, the absorption length of the tube is 5 ft (1.5 m) and the tube diameter is 0.75 in. (19 mm). To determine the mass absorbed, by conservation of the Libr:

$$\dot{m}_{soln,out}=\frac{\omega_{B\,in}}{\omega_{B\,out}}\dot{m}_{soln,in}, \tag{54}$$

where $\omega_{B\,in}$ is the bulk mass fraction at the entrance and $\omega_{B\,out}$ is the corresponding quantity at the exit. Thus the total mass absorbed is given by:

$$\dot{m}_{abs}=\dot{m}_{soln,out}-\dot{m}_{soln,in}. \tag{55}$$

On Figures 2 through 8, the properties and flow parameters are as on data set 1 of Table 1, except for the flow rate as noted. On Figure 2 are temperature profiles across the film for various values of z for the case of constant wall temperature for the inlet flux 3.728 kg/min. In this case $\lambda_1=1.62$ and the convective terms in the energy equation are $O(1)$. On Figure 2(a) are results at $z=0.0025$, 0.005, 0.0075, and 0.01. There is a discontinuity at $z=0$ due to the difference $\Delta T=T_{sin}-T_{win}>0$. However, as z increases, because of the very slow variation in film thickness, the temperature variation across the tube becomes conduction dominated. On Figure 3 are the corresponding results for the variable wall temperature, Eq. 51, with an increasing wall temperature ($\Delta T_{wall}=+4$ K). On Figure 4 are the results corresponding to a flow rate of 0.3728 kg/min for the constant wall temperature and note that the temperature distribution is conduction driven at a much earlier stage than for the higher flow rate case (compare with Figure 2(a)); on this Figure $\lambda_1=0.075$. On Figure 5 are the corresponding results for the variable wall temperature and a flow rate of 0.3728 kg/min.

The dimensionless film surface temperature for $\lambda_1=0.075$ is depicted in Figure 6 for both the case of constant and variable wall temperatures. Even though the result for the constant wall temperature appears to vary significantly in these dimensionless variables, the temperature difference corresponds to only about 8 K over 1.5 m which is much milder than the corresponding gradient across the film. In Figure 7 is the result for h_1 for the same parameters as in Figure 6. Here note the nonlinear increase in the film thickness although, on an absolute scale, the variation is indeed small. Least-squares fits of these curves reveals that a good approximation to h_1 is

$$h_1=2.526z^{0.661}, \tag{56}$$

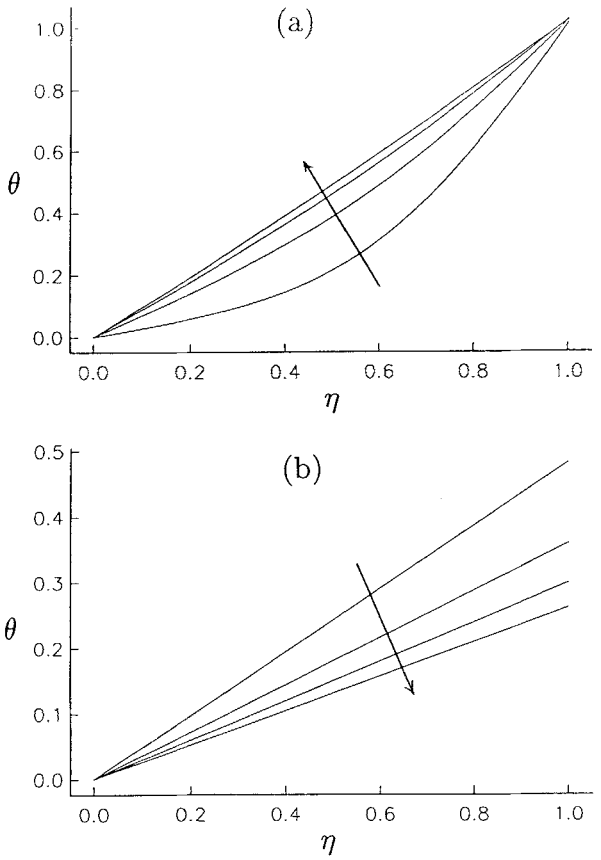

Figure 4. Dimensionless temperature distribution across the film for various values of z: flow rate = 0.3728 kg/min.

Other parameters are for data set 1 of Table 1. The wall temperature is constant. (a) $z = 0.0025$, 0.005, 0.0075, 0.01, and (b) $z = 0.25$, 0.5, 0.75, 1.0. Arrow denotes direction of increasing z.

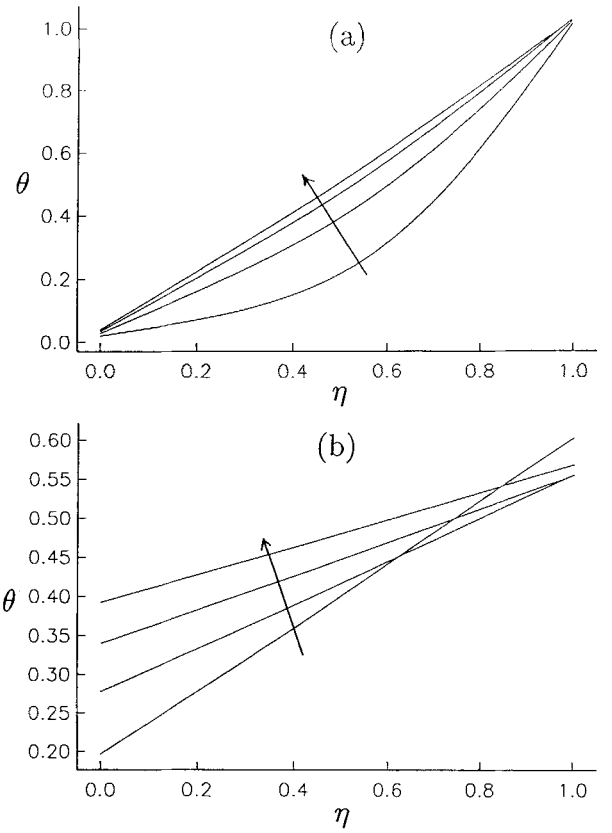

Figure 5. Dimensionless temperature distribution across the film for various values of z: flow rate = 0.3728 kg/min.

Other parameters are for data set 1 of Table 1. The wall temperature is variable according to Eq. 51 with $\Delta T_{wall} = 4$ K. (a) $z = 0.0025$, 0.005, 0.0075, 0.01, and (b) $z = 0.25$, 0.5, 0.75, 1.0. Arrow denotes direction of increasing z.

for constant wall temperature, and

$$h_1 = 2.117 z^{0.596} \tag{57}$$

for the variable wall temperature (from Eq. 51), with $\Delta T_{wall} = +4$ K.

The mass flux results for the constant wall temperature and the variable wall temperature denoted by Eq. 51 for data set 1 are depicted in Figure 8. Here we note the algebraic singularity in $\dot{m}_{a0}$ due to the form of the film thickness variation given in Eqs. 56 and 57; however, the singularity is integrable and the total mass absorbed may be obtained analytically directly from the curve fits given above or directly from the numerical solution.

At the initial writing of this article, no data on the wall temperature distribution was available. However, recently wall temperature data has been calculated by Perez-Blanco (1992) and based on the information provided by Professor Perez-Blanco, it emerges that Eq. 51 is a good representation of the wall temperature in the experiments for data sets 2 and 3. On Table 2 are the results for constant wall temperature and for the variable wall temperature given by Eq. 51. Here, the parameter ΔT_{wall} is determined by direct comparison with the information provided by Perez-Blanco (1992). Using a system approach, Perez-Blanco (1992) is able to calculate the required wall temperature given the experimental data provided by Miller. For the results of Table 2, $\Delta T_{wall} = -7$ K, for both data

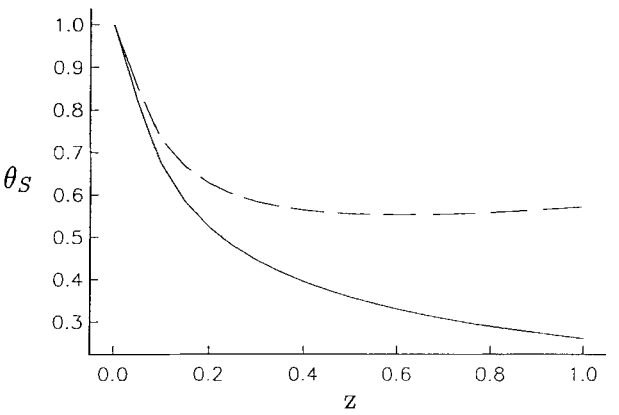

Figure 6. Dimensionless interface temperature distribution.

The solid line is for constant wall temperature and the dash line is for the variable wall case corresponding to Eq. 51 for $\Delta T_{wall} = 4$ K. The flow rate is 0.3728 kg/min. Other parameters are for data set 1 of Table 1.

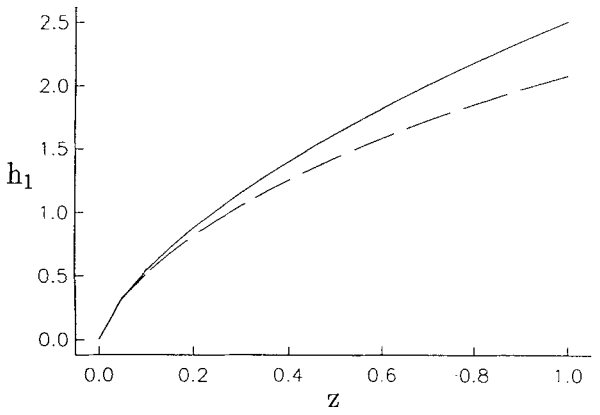

Figure 7. Dimensionless leading order film thickness variation, h_1.

The solid line is for constant wall temperature and the dash line is for the variable wall case corresponding to Eq. 51 for $\Delta T_{wall} = 4$ K. The flow rate is 0.3728 kg/min. Other parameters are for data set 1 of Table 1.

sets 2 and 3. The wall temperature distribution for data set 1 exhibits a rapid rise near the entrance of the tube before decreasing down the tube; this variation cannot be represented well with the distribution given by Eq. 51 and thus data set 1 is not considered here. This data set will be considered in future work. Note the general good agreement of the predicted results with the data for the given variable wall temperature. There does seem to be a significant discrepancy between the predicted bulk temperature and the experimental bulk temperature for data set 2 for the variable wall temperature case; however the mass-transfer quantities still appear well predicted. The reason for this discrepancy is unknown; however, see the discussion below.

In Figure 9 are the results for the film thickness h_1; the top figure includes points very near the entrance from $z = 0.0025$ to $z = 0.025$. The bottom figure is for $z = 0.025$ to $z = 1$. Note that over most of the film, the film thickness for data set 3 increases linearly. However, very near the entrance, the variation again appears to be of the form z^γ with $\gamma < 1$. This behavior is reflected in the plots of the mass flux given in Figure 10. Here the same format as in Figure 9 is followed with the top figure denoting the regime from $z = 0.0025$ to $z = 0.025$ and the bottom figure denoting the regime $z = 0.025$ to $z = 1$. Note the extremely rapid variation of the mass flux near the entrance indicating that an algebraic singularity is present in both data sets. However, the computational scheme has no difficulty in resolving these steep gradients; additional computations for even smaller z indicates that there are no numerical instabilities in the solution as may occur in other methods (Grossman (1983), Vliet (1983)). It is useful to plot the wall, bulk and film surface temperature as a function of

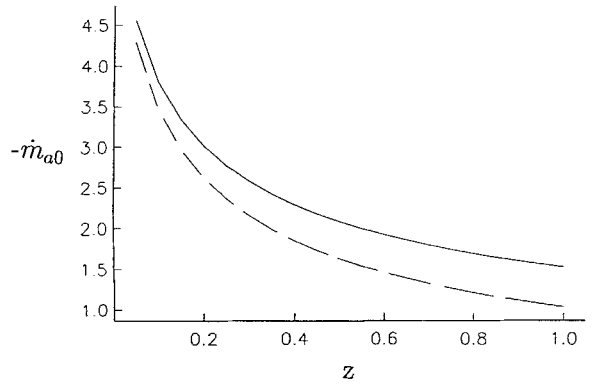

Figure 8. Dimensionless leading order mass flux at the interface $-\dot{m}_{a0}$.

The solid line is for constant wall temperature and the dash line is for the variable wall case corresponding to Eq. 51 for $\Delta T_{wall} = 4$ K. The flow rate is 0.3728 kg/min. Other parameters are for data set 1 of Table 1.

Table 2. Results for Wall Temperature of Eq. 51

Data Set	2	3
Average Mass Fraction libr Out		
Experiment	0.5404	0.6104
Theory	0.5359	0.6082
Theory (CWT)	0.5451	0.6200
Average Temperature Out		
Experiment	308.13	322.94
Theory	301.64	320.82
Theory (CWT)	307.81	327.15
Mass Absorbed (kg/min)		
Experiment	0.0213	0.0092
Theory	0.0257	0.0107
Theory (CWT)	0.0167	0.0035

For both data sets, $\Delta T_{wall} = -7$ K. CWT refers to the case of constant wall temperature. No free constants are used in the comparisons.

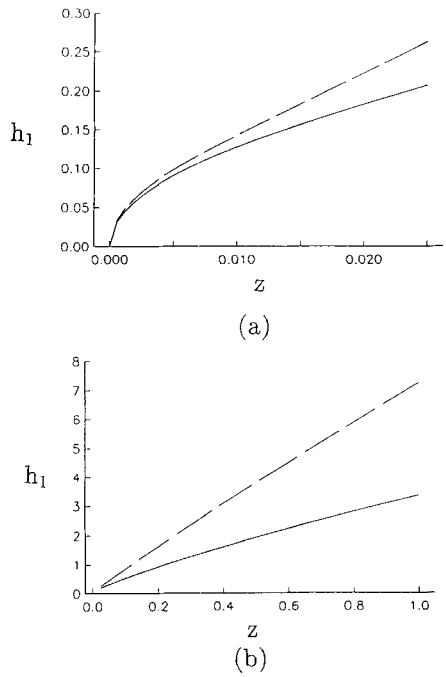

Figure 9. Dimensionless leading order film thickness variation, h_1 for the wall temperature distribution given by Eq. 51.

The solid line is for data set 2 and the dash line is for data set 3. (a) $0.0025 \le z \le 0.025$; and (b) $0.025 \le z \le 1$.

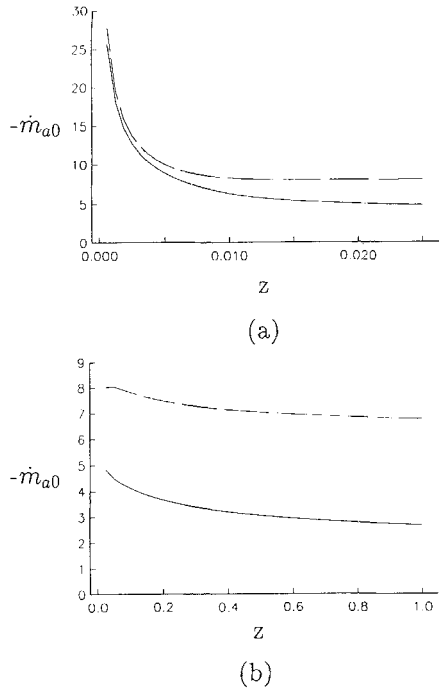

Figure 10. Dimensionless leading order mass flux at the interface $-\dot{m}_{a0}$.

The solid line is for data set 2 and the dash line is for data set 3. (a) $0.0025 \le z \le 0.025$; (b) $0.025 \le z \le 1$.

z; in Figure 11 are the results for data sets 2 and 3 and note the asymptotic decrease in the temperature difference between the wall and the surface.

In summary, the mass-transfer quantities of interest such as total mass flux and average mass fraction appear to be well predicted by the present theory. The average bulk temperature does not appear to be well predicted in the case of data set 2. This problem may be resolved by direct measurement of the wall temperature distribution which will be done shortly (Miller, 1992); in addition, the presence of waves on the film may be a contributing factor as well (see below).

Summary and Conclusions

In the present work we have formulated and solved the problem of absorption of a single fluid into a falling film binary mixture. For simplicity, one of the components of the binary mixture has been assumed to be inert. Results have been produced for a lithium-bromide-water mixture which has been employed in a variety of industrial applications. The flow and heat- and mass-transfer problems have been formulated and solved in the thin film limit ($\epsilon Re \ll 1$) and in the thick film or boundary layer limit ($\epsilon Re = 0(1)$). For both parameter ranges, it has been argued that the flow problem is solved using the Nusselt solution; the mass-transfer problem possesses closed form analytical solutions in both ranges as well. For the boundary layer limit the heat-transfer problem also possesses a closed form solution.

In the general case, the film surface temperature and mass fraction are both unknown. They are determined by applying the condition of equilibrium which relates the surface temperature to the surface mass fraction. Because of the large liquid side mass-transfer resistance, the film thickness to leading order is constant; in the boundary layer limit, the leading order film thickness, while small has the typical $z^{1/2}$ boundary

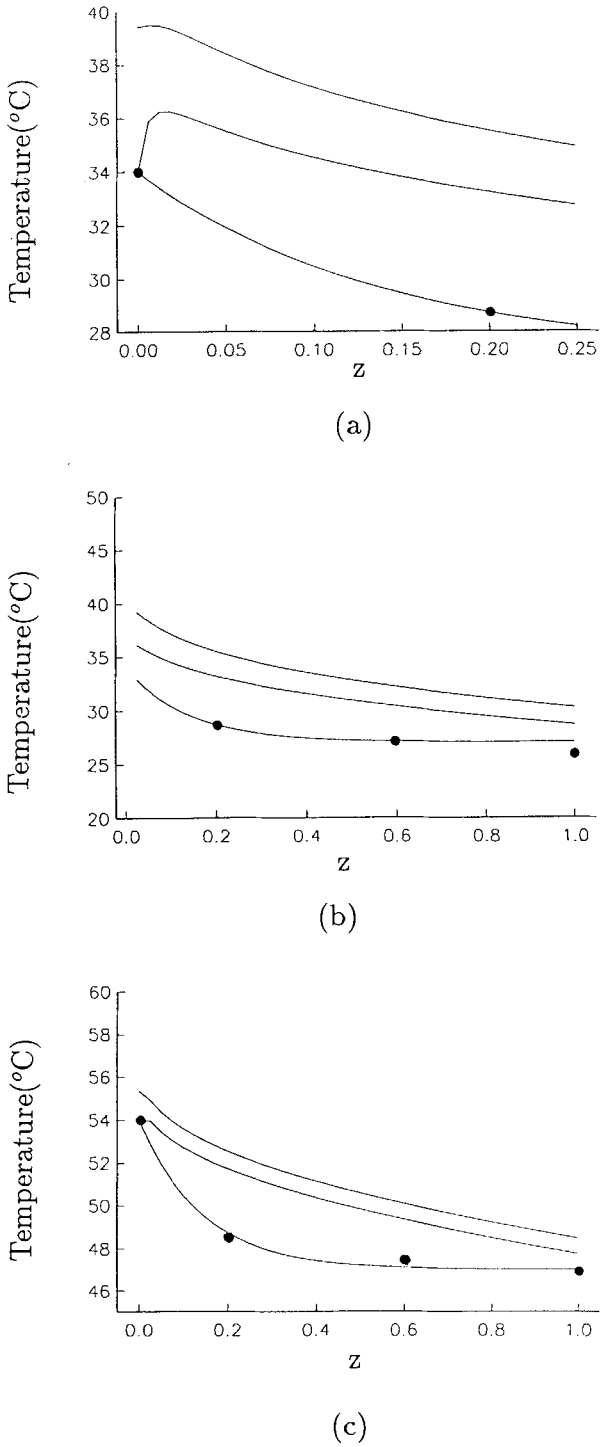

Figure 11. Film surface temperature (highest), bulk temperature, and wall temperature for the parameters of data sets 2 and 3.

(a) Data set 2 for small z, (b) data set 2 for the entire length, and (c) data set 3. The • denotes the calculated wall temperature values provided by Perez-Blanco (1992).

layer behavior. For the case of $\epsilon RePr = 0(1)$, the film thickness has similar behavior.

The theoretical results have been compared with a set of experimental data taken recently by Miller (1991) (see also Miller et al., 1992). Primary focus has been on the comparison of the outlet average mass fraction and the mass of vapor absorbed. The comparisons have been shown to be good. Moreover, all the relevant comparisons may be done analytically with little numerical work, thus defining a very simple design procedure valid for a wide range of physical parameters. Indeed, there is evidence to suggest that the use of Eq. 46 for the temperature distribution does not lead to substantial errors in the prediction of the total mass absorbed into the film.

The present work has made use of the fact that significant mass transfer takes place only in a thin layer near the liquid-vapor interface. This layer is much thinner than the corresponding heat-transfer boundary layer [$Le \ll 1$; $\epsilon Re = 0(1)$]. The absorption of vapor has been shown to be controlled by a mass-transfer driving parameter which is small in the present context. Using this parameter (B), the concept of a liquid-side mass-transfer resistance has been identified; a possible definition of a resistance, from Eq. 31 is:

$$R_M = \frac{1}{\delta^{1/2} B}$$

which is very large for both δ and B small as is the case here.

The approach taken in the present work is much different than that of earlier work on this problem. In the work of Andberg and Vliet (1983) numerical solutions are obtained for both the temperature and mass fraction distributions and the leading order variation in the film thickness is not calculated. Mass transfer takes place over the entire film because the flow rate is very low and in the present notation $\delta = 0(1)$. For this reason comparison of the work of Andberg and Vliet (1983) with the results of the present boundary layer analysis is not appropriate.

The present results are qualitatively similar to those of the Grossman (1983) constant wall temperature results for values of the axial coordinate $\zeta = z/(RePrh_0^*)$ in the present notation between 0.1 and 10. In particular, the film surface temperature decreases as a function of axial distance down the tube in a manner similar to that of Figures 2, 6 and 8 of Grossman (1983). In addition, it should be noted that the boundary layer character of the present work is also evident in the Grossman (1983) article; indeed he mentions this fact in the discussion of Figure 5 of his work. The cross-stream temperature profile quickly becomes conduction-dominated as in the present work. The variation of the dimensionless mass flux in the present work is consistent with the Grossman (1983) results as well. Critical to a quantitative comparison is operating pressure and temperature which effectively determine the constants C_1 and C_2, the Grossman scaling parameters C_e, C_0, T_e and T_0 and the flow rate; the values of these parameters at which the results are presented are not obvious.

The calculation of the leading order film variation is important, because of the film gradient is proportional to the amount of vapor absorbed on the tube. Moreover, the numerical solution procedure described in the two references makes the development of a simple design procedure more difficult. In the present work, analytical solutions may be obtained for all quantities of interest, except for the temperature in the case $\epsilon RePr = 0(1)$. This leads to a simple expression for the leading order film thickness, the absorption capacity and the average mass fraction, thus leading to a design procedure which may be performed, essentially analytically. However, the present solutions are only valid for $(\epsilon ReSc)^{-1} \ll 1$; for the parameters of Miller (1991), the mass-transfer layer will be small only for $L \leq 3$ m.

It remains to consider the effect of waves on the mass-transfer process. It is well known that a laminar film may exhibit a wavey character for a Reynolds number, based on mass-flow rate of about 30 (Dukler, 1972); it is also well known that such a process may significantly enhance the mass-transfer process (Emmert and Pigford, 1954; Javdani, 1974; Ruckenstein and Berbente, 1974). As mentioned earlier, Uddholm and Setterwall (1988) consider wavey film flow; their results suggest that the effect of the waves on the heat-transfer process is substantial and imply without proof that the mass-transfer process is significantly affected as well. The Reynolds number range of interest is unclear.

A more quantitative approach had been taken much earlier by Javdani (1974). Javdani (1974) suggests that the enhancement effect, based on a significant increase in the Sherwood number is a function of a single dimensionless variable. In the present notation, this variable is proportional to $E\delta^{1/2}$ where $E = .15\epsilon_w$, where $\epsilon_w = 1/2\alpha_w^2 A_w^2 (C_r - 3/2) Re^2 Sc$ and $\delta = 1/\epsilon ReSc$. Here α_w is the wave number of the disturbance, A_w is the dimensionless amplitude of the disturbance (based on the length L), C_r is the wave speed, and Re and Sc are as previously defined. For the present flow field, typical parameters are $\alpha_w \sim 0.1$, $C_r \sim 2$ and $A_w \sim 3 \times 10^{-4}$; the amplitude of the wave here is about twice the film thickness (Miller, 1992). For these values of the parameters, $E\delta^{1/2} \sim 1.2 \times 10^{-4}$ and using the result of Figure 4 of Javdani (1974), the direct effect of the wavy motion on the mass-transfer process appears to be small for the Reynolds number range considered.

In summary, solutions for the temperature and mass fraction in a falling liquid mixture have been calculated. A wide variety of phenomena have been observed depending on the particular wall temperature distribution. In the process, a simple design procedure has been developed; the value of the present procedure is that no free constants have been used in the course of the solution and the numerical transform method is able to resolve the very steep gradients which occur in the absorption mass flux near the entrance. The program used to calculate these solutions now takes less than 30 seconds in real time to run on a Silicon Graphics workstation and only the temperature must be calculated numerically. The agreement with experimental data is good although there is a significant discrepancy between the calculated and experimental values of the bulk temperature distribution for one of the data sets. The reason for the discrepancy is unclear; however it may be due to the presence of waves on the liquid film. Because mass transfer takes place only locally in a thin layer near the interface, it is possible that the presence of waves may substantially affect the heat transfer within the film while leaving the mass-transfer process substantially unaffected (Javdani, 1974). In addition, this issue may also be clarified by direct measurement of the wall temperature distribution which is forthcoming (Miller, 1992).

Acknowledgment

The author is grateful to Dr. Tony DeVuono for helpful discussions. The cooperation of Mr. W. A. Miller of Oak Ridge National Laboratory and Professor Horatio Perez-Blanco of Penn State in providing the experimental data for comparison is greatly appreciated. Their experimental work is funded through the Gas Research Institute. Professor Saleh Tanveer provided some helpful comments concerning the analytical solution for the temperature distribution. The numerical solution for the temperature distribution was performed by Xiao Zhenhua.

Notation

a = $\lambda_1 s/2$
B = mass-transfer driving parameter
C_1 = fit constant (Eq. 39)
C_2 = fit constant (Eq. 39)
C_p = specific heat
D_{AB} = diffusion coefficient
Fr = Froude number = gh_0^*/U_0^2
g = acceleration due to gravity
h = dimensionless film thickness
h_0^* = dimensional film thickness at the inlet
h_1 = Eq. 35
h_{abs} = heat of absorption
Ja = Jakob number = $C_p\Delta T/habs$
k = thermal conductivity
L = length of the tube
Le = Lewis number = Pr/Sc
$\dot{m}$ = dimensionless mass-flow rate
$\dot{m}^*$ = dimensional mass-flow rate
$\dot{m}_a$ = dimensionless mass absorbed
$\dot{m}_{ao}$ = scaled dimensionless mass
$\dot{m}_{abs}$ = dimensional mass absorbed (Eq. 34)
$\dot{m}_{soln,out}$ = dimensional solution mass flux out
Pr = Prandtl number
Re = Reynolds number
r_i = radius of the tube
s = Laplace Transform Variable
S_c = Schmidt number
T = temperature
T_{sin} = interface temperature at $z=0$
T_{win} = wall temperature at $z=0$
u = dimensionless velocity in the y-direction
u_0 = scaled velocity ($u=\epsilon u_0+\cdots$)
U_0 = velocity scale
w = dimensionless velocity in the z direction
y = dimensionless coordinate normal to the wall
z = dimensionless coordinate in the direction of gravity

Greek letters

α = ρ_w/ρ
β = see Eq. 40
δ = $1/(\epsilon ReSc)$
δ_1 = $1/(\epsilon RePr)$
ΔT = $T_{sin}-T_{win}$
ΔT_w = overall wall temperature difference
ϵ = h_0^*/L
η = y/h
$\overline{\eta}$ = $(1-\eta)/\delta^{1/2}$
$\hat{\eta}$ = $(1-\eta)/\delta_1^{1/2}$
θ = dimensionless temperature (Eq. 10)
θ_s = dimensionless interface temperature
θ_w = dimensionless wall temperature
λ = $\epsilon RePr$
λ_1 = $\lambda ReFr$
μ = dynamic viscosity
ν = kinematic viscosity
ξ = $1-\eta$
ρ = density of the mixture
ρ_w = density of water
ω_A = mass fraction
ω_{AS} = mass fraction at the interface
$\omega_{A\,BULK}$ = mass fraction in the majority of the film
Ω = scaled mass fraction (Eq. 28)
Ω_s = scaled interface mass fraction
Ω_{AVE} = average mass fraction

Literature Cited

Acrivos, A., "The Asymptotic Form of the Laminary Boundary Layer Mass Transfer Rate For Large Interfacial Velocities," *J. Fluid Mech.*, **12**, 337 (1962).

Andberg, J. W., and G. C. Vliet, "Nonisothermal Absorption of Gases into Fall Liquid Films," *ASME-JSME Joint Thermal Engineering Conf.*, **2**, 423 (1983).

Bird, R. B., W. E. Stewart, and E. N. Lightfoot, *Transport Phenomena*, Wiley, New York (1960).

Buffington, R. M., "Qualitative Requirements for Absorbent-Refrigerant Combinations," *Refrig. Eng.*, **57**, 343, 384 (Apr., 1949).

Colburn, A. P., and T. B. Drew, "The Condensation of Mixed Vapors," *Trans. AIChE*, **33**, 197 (1937).

Dukler, A. E., "Characteristic Effects and Modeling of the Wavy Gas-Liquid Interface," in *Prog. Heat Mass Transfer*, **6**, 207 (1972).

Emmert, R. E., and R. L. Pigford, "A Study of Gas Absorption in Falling Liquid Films," *Chem. Eng. Prog.*, **50**, 87 (1954).

Gradsteyn, I. S., and I. M. Ryzhik, *Table of Integrals, Series, and Products*, p. 1067, Academic Press (1980).

Grigor'eva, N. I., and V. E. Nakoryakov, "Exact Solution of Combined Heat and Mass Transfer Problem During Film Absorption," *J. Eng. Physics*, **33**(5), 1349 (1977).

Grossman, G., "Simultaneous Heat and Mass Transfer in Film Absorption Under Laminar Flow," *Int. J. Heat Mass Transfer*, **26**(3), 357 (1983).

Grossman, G., "Analysis of Interdiffusion in Film Absorption," *Int. J. Heat Mass Transfer*, **30**(1), 205 (1987).

Honig, G., and U. Hirdes, "A Method for the Numerical Inversion of Laplace Transforms," *J. Comp. Appl. Math.*, **10**, 113 (1984).

Javdani, K., "Mass Transfer in Wavy Liquid Films," *Chem. Eng. Sci.*, **29**, 61 (1988).

Merk, H. J., "Mass Transfer in Laminar Boundary Layers Calculated by Means of Perturbation Method," *Appl. Sci. Res A*, **8**, 237 (1959).

Miller, W. A., Private Communication (1991, 1992).

Miller, W. A., H. Perez-Blanco, and W. Ryan, "Coupled Heat and Mass Transfer in Falling Film Absorption of an Aqueous Lithium-Bromide Solution Under Laminar Flow," ASME Winter Annual Meeting, Los Angeles (Nov., 1992).

Olbrich, W. E., and J. D. Wild, "Diffusion From a Free Surface into a Liquid Film in a Laminar Flow Over Defined Shapes," *Chem. Eng. Sci.*, **24**, 25 (1969).

Perez-Blanco, H., Private Communication (1992).

Rotem, A., and J. E. Neilson, "Exact Solution for Diffusion to Flow Down an Incline," *Can. J. Chem. Eng.*, **47**, 341 (1969).

Ruckenstein, E., and C. Berbente, "Mass Transfer to Falling Liquid Films at Low Reynolds Numbers," *Int. J. Heat Mass Transfer*, **11**, 743 (1968).

Sparrow, E. M., and E. Marschall, "Binary, Gravity-Flow Film Condensation," *ASME J. Heat Transfer*, **91**, 205 (1969).

Tamir, A., and Y. Taitel, "Diffusion to Flow Down and Incline With Surface Resistance," *Chemical Eng. Sci.*, **26**, 799 (1971).

Uddholm, H., and F. Setterwall, "Model for Dimensioning a Falling Film Absorber in an Absorption Heat Pump," *Int. J. Ref.*, **11**, 41 (Jan., 1988).

van der Wekken, B. J. C., and R. H. Wassenaar, "Simultaneous Heat and Mass Transfer Accompanying Absorption in Laminar Flow Over a Cooled Wall," *Int. J. Ref.*, **11**, 70 (Mar., 1988).

Manuscript received Jan. 24, 1992, and revision received June 19, 1992.